Polymer Chemistry

Accepted Manuscript

This is an *Accepted Manuscript*, which has been through the Royal Society of Chemistry peer review process and has been accepted for publication.

Accepted Manuscripts are published online shortly after acceptance, before technical editing, formatting and proof reading. Using this free service, authors can make their results available to the community, in citable form, before we publish the edited article. We will replace this *Accepted Manuscript* with the edited and formatted *Advance Article* as soon as it is available.

You can find more information about *Accepted Manuscripts* in the Information for Authors.

Please note that technical editing may introduce minor changes to the text and/or graphics, which may alter content. The journal's standard Terms & Conditions and the Ethical guidelines still apply. In no event shall the Royal Society of Chemistry be held responsible for any errors or omissions in this *Accepted Manuscript* or any consequences arising from the use of any information it contains.

ROYAL SOCIETY OF CHEMISTRY

www.rsc.org/polymers

Polymer Chemistry

ARTICLE

Influence of Regiochemistry in the Selective Dispersion of Metallic Carbon Nanotubes Using Electron Poor Conjugated Polymers

Received 00th January 20xx,
Accepted 00th January 20xx

DOI: 10.1039/x0xx00000x

www.rsc.org/

W. J. Bodnaryk, N. A. Rice, and A. Adronov*

The incorporation of single walled carbon nanotubes (SWNTs) into electronic devices requires electronically pure samples of either semiconducting or metallic SWNTs. Selective extraction of SWNTs by wrapping with electron-rich conjugated polymers has proven an effective method for producing samples enriched in semiconducting SWNTs. However, large-scale purification of metallic SWNTs with conjugated polymers has proven elusive. Here, we report SWNT dispersions prepared with three structurally similar poly(fluorene-*co*-phenylene) derivatives that possess varying degrees of nitration on the fluorene monomers. Differentiation of semiconducting and metallic SWNT populations was carried out by a combination of UV-Vis-NIR absorption, Raman, and fluorescence spectroscopy. We found that copolymers with meta-substituted nitro groups (with respect to the phenylene component) exhibit minimal inductive effects on the overall polymer backbone. When the nitro groups are ortho-substituted, a significant inductive effect occurs on the polymer backbone, resulting in a polymer that is more selective toward metallic SWNTs. The assessment of the inductive effects on the copolymer species was confirmed using Density Functional Theory (DFT) calculations. These results provide new insight into polymer design features, leading to the eventual goal of a conjugated polymer capable of selectively dispersing metallic SWNTs.

Introduction

Single-walled carbon nanotubes (SWNTs) have received significant attention due to their exceptional mechanical, optical, and electronic properties.[1–4] In particular, the electrical conductivity of SWNTs, which ranges from semiconducting to metallic depending on the chiral index (n,m) of each tube,[5–7] opens numerous opportunities for applications. SWNT-based transistors,[8] sensors,[9,10] photovoltaics,[11,12] touch screens,[13] and various flexible electronics[14] have been reported, and take advantage of their unique conductivity properties. However, despite significant progress toward their commercialization,[15] the extent to which nanotubes have been incorporated within commercial products has lagged behind expectations. This is partly because all current SWNT synthetic methodologies (including chemical vapor deposition (CVD),[16,17] laser ablation,[18] arc discharge,[19] and plasma torch growth[20]) result in the production of electronically heterogeneous samples. One third of raw SWNT samples exhibit metallic conductivity (m-SWNTs), with the remaining two thirds possessing semiconducting (sc-SWNTs) characteristics.[21] This mixture in as-produced SWNTs remains a challenging barrier for applications, as many devices require either pure m-SWNTs (electrodes,[22] interconnects[23]) or pure sc-SWNTs (field-effect transistors,[24] chemical sensors[25,26]). Therefore, SWNT purification continues to be an area of intense research.[27,28]

Recently, a number of purification methods for SWNTs have been shown effective, including density gradient ultracentrifugation (DGU),[29] agarose gel filtration,[30] and electrophoresis.[31] While these methods are capable of separating metallic and semiconducting species, they are challenging to scale to industrial levels at reasonable cost, and can currently only yield minute quantities of electronically pure materials. An alternative method of nanotube purification involves supramolecular functionalization and dispersion by conjugated polymers (CPs). The broad structural versatility of CPs allows precise tuning of their properties to enable selective interactions with specific subsets of SWNTs. In addition, large-scale synthesis of CPs is feasible and cost effective, making this approach potentially scalable to industrial levels. It has been shown that many CPs exhibit selective interactions with sc-SWNTs, and some are capable of dispersing narrow chirality distributions. Polyfluorenes,[27] polycarbazoles,[32] polythiophenes,[33] and a number of other conjugated aromatic polymers have successfully been shown to selectively disperse specific SWNT types.[34,35] However, the exact structural features that control selectivity for specific SWNT chiralities are poorly understood.[36]

[a] *Department of Chemistry, McMaster University, Hamilton, Ontario L8S 4L8, Canada.*

Electronic Supplementary Information (ESI) available: Full experimental details, full characterization of the polymers prepared (including ^{1}H NMR ^{13}C NMR, and UV-Vis absorbance), as well as additional DFT and spectral data of polymer-SWNT suspensions.
. See DOI: 10.1039/x0xx00000x

We have recently begun to investigate the interactions of electron-rich (e-rich) and electron-poor (e-poor) CPs with SWNTs.[37] By preparing a series of polymers with nearly identical length and side-chain structure, but differing in the electron-withdrawing character of appended functional groups, we have shown that e-rich CPs exhibit preferential selectivity for semiconducting SWNTs, while e-poor CPs are much more selective for metallic SWNTs. Although the selectivity of e-rich CPs for semiconducting SWNTs has been reported numerous times,[38] the preference of e-poor polymers for m-SWNTs has received little attention, and therefore warrants further investigation. In particular, it is instructive to compare structurally similar polymers that are systematically modified to vary the electronic character of their backbone.

Electron-rich polyfluorenes, such as poly(9,9-dioctylfluorenyl-2,7-diyl) (PFO) have recently been shown to form strong interactions with SWNTs.[35] A number of reports have clearly shown that this CP backbone can exhibit selectivity for sc-SWNTs.[35,39,40] However, the underlying reason for this selectivity has not been clearly determined. Several variables, including molecular weight, side-chain length, and electronic character can play a role in dictating the selectivity of this CP backbone.[32,39] We hypothesize that the electronic character of the polymer backbone is a dominant factor in dictating selectivity for sc-SWNTs versus m-SWNTs. Thus, we set out to vary the extent of e-rich character of the polyfluorene backbone, while keeping the polymer molecular weight and side-chain structure constant. To achieve the desired gradient in e-rich character, the inherently e-rich fluorene monomer can be depleted of electron density via functionalization with electron-withdrawing groups. Here we describe the nitration of the fluorene monomer to different extents, followed by polymerization to produce a series of CPs that systematically differ in the number of nitro functionalities within each repeat unit. We demonstrate for the first time that it is not only the extent of nitration, but also the position of the nitro groups that dictates the electronic character of the polymer backbone and its selectivity for certain SWNT types. Specifically, conversion of the polyfluorene-*co*-phenylene backbone from one that is e-rich to one that is e-poor has a significant impact on the polymer's ability to interact with m-SWNTs.

Results and Discussion

Two nitrated fluorene monomers were prepared by first brominating commercially-available fluorene to produce 2,7-dibromofluorene (**1**), followed by alkylation to produce a monomer bearing solubilizing hexadecyl chains (**2**), as shown in Scheme 1. Nitration of the alkylated dibromide **2** to varying extents was carried out by treatment with acetic and nitric acids at different temperatures.[41] Stirring **2** with the acid mixture in CH_2Cl_2 at room temperature for 6 h resulted in the

Scheme 1. Synthesis of fluorene monomers.

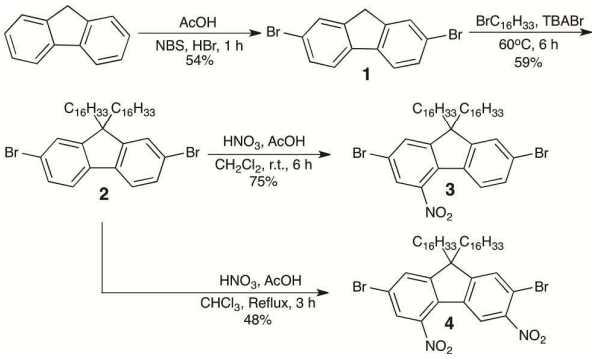

mono-nitrated 2,7-dibromo-9,9-dihexadecyl-4-nitrofluorene **3**. Alternatively, heating the same mixture in $CHCl_3$ to reflux for 3 h resulted in formation of the di-nitrated 2,7-dibromo-9,9-dihexadecyl-3,5-dinitrofluorene **4** (Scheme 1). With these two monomers (**3** and **4**) and the non-nitrated analog **2** in hand, their copolymerization with 1,4-benzene diboronic acid bis(pinacol) ester as the co-monomer via Suzuki polycondensation was carried out using $Pd((o\text{-tol})_3P)_2$ as the catalyst (Scheme 2).[42] The resulting three polymers, which included the non-nitrated control poly(fluorene-*co*-phenylene) along with the mono-nitrated and di-nitrated analogs (PF-P_{25}, PMNF-P_{25}, and PDNF-P_{23}, respectively) were isolated in good yield as solid powders which ranged in color from white (PF-P_{25}) to yellow (PMNF-P_{25}) and green (PDNF-P_{23}). All three polymers were soluble in common organic solvents, including THF, toluene, and chloroform. Gel permeation chromatography (GPC) was used to assess the molecular weight of the three isolated polymers (Table 1), which were all very similar in their M_n and polydispersity values. Keeping the molecular weights of each of the three polymers constant was critical to enabling robust comparison of their relative ability to interact with specific SWNT types.

Supramolecular complexes between each of the three polymers with raw HiPCO SWNTs were prepared following previously reported procedures.[43] Briefly, 10 mg of SWNTs

Scheme 2. Synthesis of the three fluorene-*co*-phenylene copolymers.

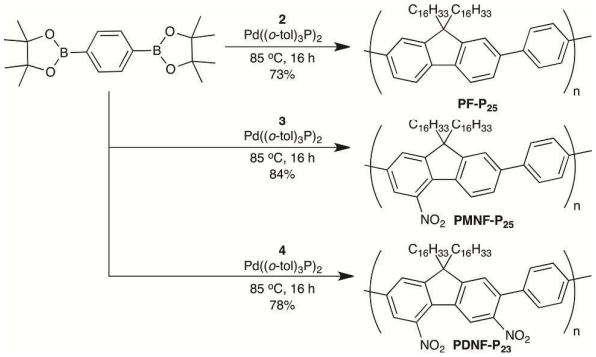

were added to solution of 15 mg of polymer dissolved in 20 mL of a 1:1 THF:toluene (v/v) co-solvent mixture. This solvent mixture was found to be optimal in achieving well exfoliated and stable SWNT dispersions. The sample was sonicated for 2 h in an ice-chilled bath sonicator, followed by centrifugation at 8,346 *g* for 30 min. The supernatant was then removed from the centrifuge tube, filtered over a 0.2 µm PTFE membrane, and thoroughly rinsed with solvent to remove excess polymer. The nanotube residue was then redispersed in 15 mL of solvent, followed by a second sonication and centrifugation step.

Table 1: Yield and molecular weight data for PF-P_{25}, PMNF-P_{25}, and PDNF-P_{23} copolymers.

Polymer	Yield	M_n (kDa)	M_w (kDa)	PDI	DP
PF-P_{25}	73%	25.4	53.8	2.12	37
PMNF-P_{25}	84%	25.4	53.5	2.11	35
PDNF-P_{23}	78%	23.3	48.9	2.09	30

To characterize the polymer-SWNT complexes, we first performed UV-Vis-NIR absorption spectroscopy (Figure 1). The multiple observed absorption peaks arise from the various SWNT chiralities present within the dispersions. There are three different regions of interest in the absorption range investigated, including two semi-conducting regions, S_{11} (830-1600 nm) and S_{22} (600-800 nm), and one metallic region, M_{11} (440-645 nm).[44] PF-P_{25}-SWNT and PMNF-P_{25}-SWNT show very similar absorption features, with the relatively intense peaks in the S_{11} and S_{22} regions suggesting that exfoliated sc-SWNTs are dispersed by these two polymers. Thus, both polymers disperse similar populations of sc-SWNTs, except for one intense peak corresponding to the (8,7) chirality observed with PF-P_{25}-SWNT (at ca. 1284 nm) PDNF-P_{23}-SWNT also shows absorption peaks in the S_{11} and S_{22} regions, but they are significantly broader and there is a noticeable exponential background. These features, coupled with the presence of absorption peaks in the M_{11} region, are indicative of the presence of m-SWNTs in the PDNF-P_{23}-SWNT suspension.[44]

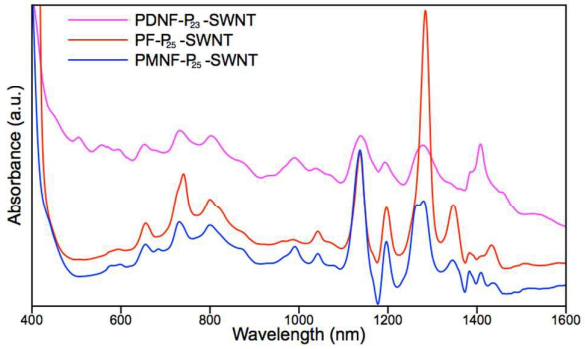

Figure 1. UV-Vis-NIR absorbance data for PF-P_{25}-SWNT (red), PMNF-P_{25}-SWNT (blue), and PDNF-P_{23}-SWNT (magenta) in 1:1 THF:Tol. Absorbance data has been vertically offset for clarity.

Resonance Raman spectroscopy was performed to further investigate the m-SWNT and sc-SWNT populations dispersed by the three different polymers. Raman spectroscopy is a valuable technique for discriminating the diameter of dispersed SWNTs (based on positions of radial breathing mode (RBM) signals in the 100-400 cm^{-1} range),[45] as well as the relative amounts of of both metallic and semiconducting SWNTs present in a sample, which are separately probed using different excitation wavelengths.[46] Polymer-SWNT thin film samples were prepared by drop-casting the suspensions onto silicon wafers and allowing the solvent to evaporate. A reference SWNT sample was also prepared by sonicating the raw HiPCO SWNT starting material in chloroform and using this suspension to prepare a thin film using the same drop-casting method. Raman experiments were performed using three different excitation wavelengths: 514, 633, and 785 nm. While three excitation wavelengths are not sufficient to fully characterize all the SWNT populations present, it has been previously demonstrated that using these three wavelengths allows adequate discrimination of the electronic nature of HiPCO SWNTs.[45] Figure 2 shows Raman data, focusing on the RBM region, for the three polymer-SWNT samples excited at the three different wavelengths. All spectra were normalized to the G-band (at approximately 1590 cm^{-1}) for comparative analysis, and offset for clarity. Full Raman spectra can be found in the Supporting Information.

For HiPCO SWNTs, the peaks observed in the RBM using the 514 nm excitation wavelength can be grouped into two regions (Figure 2A): a broad, low-intensity peak centered at 180 cm^{-1} arising from sc-SWNTs, and several intense peaks between 225 and 290 cm^{-1} arising from m-SWNTs.[47] Although both semiconducting and metallic features are present for all three polymer-SWNT samples, the metallic features are most pronounced in the PDNF-P_{23}-SWNT spectrum. This is corroborated by analysis of the G-band region at this excitation wavelength, shown in the inset of Figure 2A. The G-band is split into two components: the high frequency G^+ and the lower frequency G^-. With sc-SWNTs, both the G^+ and G^- exhibit Lorentzian-style lineshapes, whereas with m-SWNTs the G^+ remains Lorenztian but the G^- displays a broader Breit-Wigner-Fano (BWF) lineshape.[48] The BWF lineshape is observed in the G^- for PDNF-P_{23}-SWNT, but is not evident for PF-P_{25}-SWNT and PMNF-P_{25}-SWNT, suggesting that the latter are not highly selective for m-SWNTs.

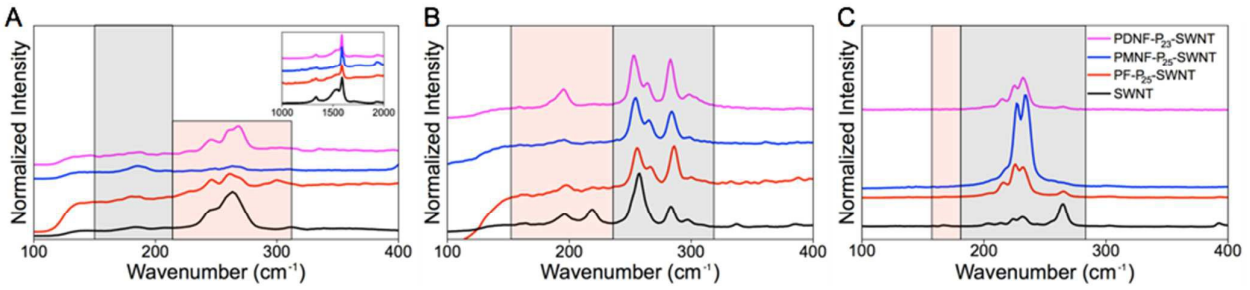

Figure 2. Raman spectra showing RBM regions obtained using (A) 514, (B) 633, and (C) 785 nm excitation wavelengths. The pink box represents locations of signals arising from m-SWNTs, while the grey regions represent sc-SWNTs. The inset in (A) shows the G-band region, upon excitation at 514 nm.

With the 633 nm excitation (Figure 2B), both metallic and semiconducting SWNTs are again in resonance, allowing both electronic types to be observed. At this excitation wavelength, HiPCO m-SWNTs can be observed in the 175-230 cm^{-1} range, while sc-SWNT features are found at 240-300 cm^{-1}.[49] Again, both m-SWNTs and sc-SWNTs are observed for all polymer-SWNT composites, but the PDNF-P_{23}-SWNT sample gave rise to the significantly more intense features in the metallic range than PF-P_{25}-SWNT and PMNF-P_{25}-SWNT. These findings support the hypothesis that decreasing electron density on the polymer backbone increases the selectivity toward m-SWNTs. The third excitation wavelength, 785 nm (Figure 2C), is mostly in resonance with sc-SWNTs. When excited at this wavelength, raw HiPCO SWNTs give rise to an intense peak at ~265 cm^{-1}, which originates from (10,2) SWNTs that are present in bundles. This peak is referred to as the "bundling peak", and allows for a qualitative evaluation of the amount of bundling present in a given suspension.[50] Figure 2C shows that all three polymer-SWNT samples exhibit minimal bundling compared to the raw nanotube control sample, suggesting that all the polymers can efficiently exfoliate SWNTs. In addition, significant signals corresponding to sc-SWNTs are observed in the 220-250 cm^{-1} range.

PL maps for the polymer-SWNT samples were recorded and overlaid with known locations of sc-SWNT fluorescence maxima, assigned based on previous literature reports (Figure 3).[51] Both PF-P_{25}-SWNT and PMNF-P_{25}-SWNT exhibited more intense PL signals than the PDNF-P_{23}-SWNT sample. Additionally, although both PF-P_{25}-SWNT and PMNF-P_{25}-SWNT contain similar minor contributors (such as the (10,2), (8,6), and (7,5) chiralities), they differ in which chiralities give rise to the most intense fluorescence maxima; the (8,7) chirality is most intense in the PF-P_{25}-SWNT sample, while the (7,5) chirality is most intense for PMNF-P_{25}-SWNT. This is consistent with the UV-Vis-NIR results (Figure 1), and suggests that the inclusion of the nitro functionality in PMNF-P_{25}-SWNT slightly alters the populations of sc-SWNTs dispersed. Despite the presence of sc-SWNTs in the PDNF-P_{23}-SWNT sample (observed in both the absorbance and Raman results), the PL map for this sample did not show any clearly defined PL peaks. Fluorescence signals could only be observed from this sample when the intensity scale was significantly reduced (Figure 3C). The observed fluorescence quenching can be ascribed to either the dispersion of nanotube bundles by PDNF-P_{23}, or by the selective dispersion of m-SWNTs. The Raman data described above rules out the presence of nanotube bundles in this dispersion (based on the lack of a "bundling peak"), allowing us to conclude that the presence of m-SWNTs is the major source for the observed fluorescence quenching.[5,37] Therefore, the combination of Raman and UV-Vis-NIR absorption spectroscopy indicates that the di-nitrated PDNF-P_{23} is significantly more selective toward m-SWNTs than the non-nitrated PF-P_{25} or the mono-nitrated PMNF-P_{25}.

What is surprising about these results is that the mono-nitrated polymer, PMNF-P_{25}, does not exhibit intermediate selectivity for m-SWNTs between the non-nitrated and di-nitrated analogs. Instead, it behaves much more like the non-nitrated PF-P_{25}, despite the presence of a strongly electron-withdrawing nitro group on each repeat unit. As both polymers have similar molecular weights and solubilities, we propose that this anomalous behaviour could be due to one of three possibilities: the polymers may adopt significantly different conformations, the regiochemistry of the nitro group could affect its influence on polymer electronics, or the addition of the second nitro unit could be essential for inducing a significant enough change in the electronic nature of the polymer backbone.

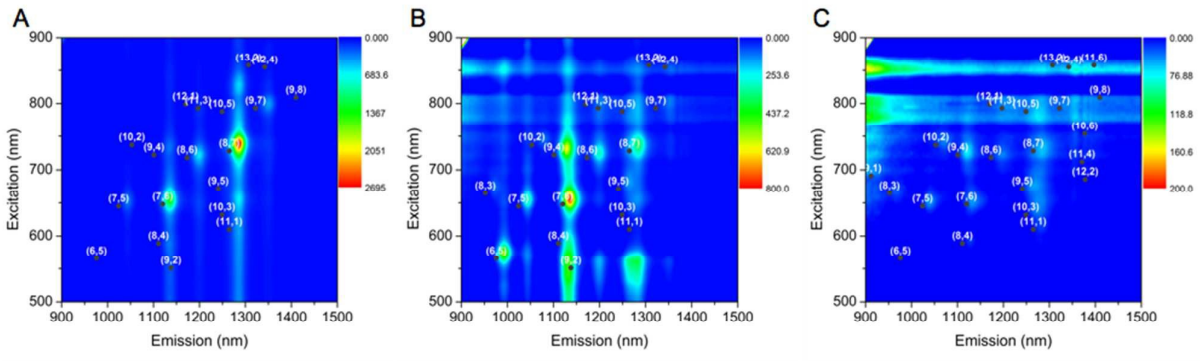

Figure 3. PL maps for (A) PF-P_{25}-SWNT, (B) PMNF-P_{25}-SWNT, and (C) PDNF-P_{23}-SWNT.

To investigate the conformations of the polymer series and the influence of the location and amounts of nitro functionalities on the electron density of the backbone, we performed Density Functional Theory (DFT) calculations (M06 functional and 6-31G(d) basis set) using the GAMESS software package (Figure 4).[52] Trimers of the three polymers used in this study, along with a mono-functionalized analog having the nitro group in the ortho position relative to the adjacent phenyl ring (*o*-PMNF-P), were computationally investigated. We found that despite increasing the number of nitro functionalities on the polymer backbone, the conformation of the polymers remain comparable, which suggests that the difference in observed suspension selectivity is not due to polymer conformation. The calculated electron density maps, shown in Figure 4, are colour-coded to highlight electron-rich regions in red and electron-poor regions in blue. These maps show that the electron density distribution along the polymer backbone of PF-P_{25} and PMNF-P_{25} are remarkably similar, despite the presence of the nitro groups located meta to the adjacent phenylene unit in PMNF-P_{25}. This suggests that a strong electron-withdrawing group in the meta position of PMNF-P_{25} has minimal inductive influence over the polymer's electronic character. In contrast, calculations for both PDNF-P_{23} and the hypothetical o-PMNF-P indicate significantly less electron density in each of these polymer structures. What is more interesting is that both the mono-functionalized (ortho-substituted) and di-functionalized (ortho and meta-substituted) polymers appear to have relatively similar electron-poor backbones. This further indicates that although incorporating a second nitro functionality may help remove additional electron density from the backbone, ortho-functionalization has a more significant impact on the overall electronics of the polymer than meta-functionalization. Our experimental and theoretical results suggest that the substitution pattern of electron-withdrawing groups introduced on the polymer backbone is important when designing polymer structures for selective dispersion of m-SWNTs.

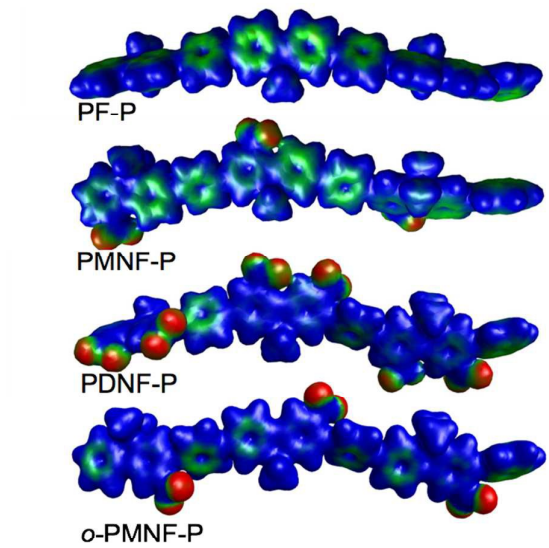

Figure 4. Electron density maps for trimers of PF-P25, PMNF-P25 (meta-functionalized), PDNF-P23 (ortho and meta-substituted), and o-PMNF-P (ortho-substituted). Red denotes regions of highest electron-density, green denotes regions of intermediate electron-density, and blue denotes regions of lowest electron-density.

Conclusions

The design of new conjugated polymers for selective dispersion of SWNTs by electronic type requires control over a number of polymer variables. Modification of the poly(fluorene-*co*-phenylene) backbone with electron-withdrawing groups has a significant effect on its interactions with specific SWNT types, demonstrating an enhanced preference for m-SWNTs. Furthermore, we have shown that the substitution pattern of the electron-withdrawing groups is important in dictating the electronic properties of the polymer backbone, and the effect on SWNT selectivity. The copolymer having a single nitro functionality in the meta position exhibited similar SWNT selectivity to a non-nitrated copolymer. However, the di-nitrated copolymer resulted in dispersions having a larger preference for m-SWNTs, mainly as a result of the ortho-substituted nitro functionality (relative to the adjacent phenyl comonomer). Understanding that the fluorene and phenylene comonomers are relatively electron

rich, it is not surprising that they are not exclusively selective towards m-SWNTs. These results justify future development of more electron-deficient polymer systems, and highlight the need for careful consideration of regiochemistry when installing electron-withdrawing functionalities that enhance the polymer's ability to selectively discriminate m-SWNTs.

Acknowledgements

Financial support for this work was provided by the Natural Science and Engineering Research Council (NSERC) of Canada. W.J.B. is grateful for support through an Ontario Graduate Scholarship (OGS). W.J.B. would like to thank Ryan C. Chadwick for extensive help with the synthesis of the monomers.

Notes and references

1 M. Yu, B. Files, S. Arepalli and R. Ruoff, *Phys. Rev. Lett.*, 2000, **84**, 5552–5.
2 Z. Han and A. Fina, *Prog. Polym. Sci.*, 2011, **36**, 914–944.
3 P. Avouris, Z. Chen and V. Perebeinos, *Nat. Nanotechnol.*, 2007, **2**, 605–615.
4 P. Avouris, *Sci. Am.*, 2000, 62–69.
5 M. J. O. Connell, S. M. Bachilo, C. B. Huffman, V. C. Moore, M. S. Strano, E. H. Haroz, K. L. Rialon, P. J. Boul, W. H. Noon, C. Kittrell, J. Ma, R. H. Hauge, R. B. Weisman and R. E. Smalley, *Science*, 2002, **593**, 593–597.
6 S. Benguediab, A. Tounsi, M. Zidour and A. Semmah, *Compos. Part B Eng.*, 2014, **57**, 21–24.
7 M. Zheng and E. D. Semke, *J. Am. Chem. Soc.*, 2007, **129**, 6084–6085.
8 T. Dürkop, S. A. Getty, E. Cobas and M. S. Fuhrer, *Nano Lett.*, 2004, **4**, 35–39.
9 B. C.-K. Tee, A. Chortos, A. Berndt, A. K. Nguyen, A. Tom, A. McGuire, Z. C. Lin, K. Tien, W.-G. Bae, H. Wang, P. Mei, H.-H. Chou, B. Cui, K. Deisseroth, T. N. Ng and Z. Bao, *Science*, 2015, **350**, 313–316.
10 K. M. Frazier, K. a Mirica, J. J. Walish and T. M. Swager, *Lab Chip*, 2014, **14**, 4059–66.
11 M. W. Rowell, M. a. Topinka, M. D. McGehee, H. J. Prall, G. Dennler, N. S. Sariciftci, L. Hu and G. Gruner, *Appl. Phys. Lett.*, 2006, **88**, 233506.
12 D. J. Bindl, N. S. Safron and M. S. Arnold, *ACS Nano*, 2010, **4**, 5657–5664.
13 D. S. Hecht, C. Ladous, P. Drzaic and S. I. D. Fellow, *J. SID*, 2009, **17**, 941–946.
14 H. Wang, P. Wei, Y. Li, J. Han, H. R. Lee, B. D. Naab, N. Liu, C. Wang, E. Adijanto, B. C.-K. Tee, S. Morishita, Q. Li, Y. Gao, Y. Cui and Z. Bao, *Proc. Natl. Acad. Sci. U. S. A.*, 2014, **111**, 4776–81.
15 M. F. L. De Volder, S. H. Tawfick, R. H. Baughman and J. A. Hart, *Science*, 2013, **339**, 535–539.
16 J. Kong, A. M. Cassell and H. J. Dai, *Chem. Phys. Lett.*, 1998, **292**, 567–574.
17 K. Bladh, L. K. L. Falk and F. Rohmund, *Appl. Phys. A Mater. Sci. Process.*, 2000, **70**, 317–322.
18 T. Guo, P. Nikolaev, A. Thess, D. T. Colbert and R. E. Smalley, *Chem. Phys. Lett.*, 1995, **243**, 49–54.
19 C. Journet, W. K. Maser, P. Bernier and a Loiseau, *Nature*, 1997, **388**, 20–22.
20 K. S. Kim, G. Cota-Sanchez, C. T. Kingston, M. Imris, B. Simard and G. Soucy, *J. Phys. D. Appl. Phys.*, 2007, **40**, 2375–2387.
21 M. M. A. Rafique and J. Iqbal, *J. Encapsulation Adsorpt. Sci.*, 2011, **1**, 29–34.
22 A. a. Green and M. C. Hersam, *Nano Lett.*, 2008, **8**, 1417–1422.
23 M. F. L. De Volder, S. H. Tawfick, R. H. Baughman and A. J. Hart, *Science*, 2013, **339**, 535–539.
24 M. Terrones, *Annu. Rev. Mater. Res.*, 2003, **33**, 419–501.
25 P. Qi, O. Vermesh, M. Grecu, A. Javey, Q. Wang, H. Dai, S. Peng and K. J. Cho, *Nano Lett.*, 2003, **3**, 347–351.
26 S. Park, M. Vosguerichian and Z. Bao, *Nanoscale*, 2013, **5**, 1727–52.
27 F. A. Lemasson, T. Strunk, P. Gerstel, F. Hennrich, S. Lebedkin, C. Barner-kowollik, W. Wenzel, M. M. Kappes and M. Mayor, *J. Am. Chem. Soc.*, 2011, **133**, 652–655.
28 E. T. Thostenson, Z. Ren and T.-W. Chou, *Compos. Sci. Technol.*, 2001, **61**, 1899–1912.
29 M. S. Arnold, A. A. Green, J. F. Hulvat, S. I. Stupp and M. C. Hersam, *Nat. Nanotechnol.*, 2006, **1**, 60–65.
30 H. Liu, T. Tanaka and H. Kataura, *J. Phys. Chem. C*, 2010, **114**, 9270–9276.
31 T. Tanaka, H. Jin, Y. Miyata and H. Kataura, *Appl. Phys. Express*, 2008, **1**, 1140011–1140013.
32 N. A. Rice, A. V. Subrahmanyam, S. E. Laengert and A. Adronov, *J. Polym. Sci. Part A Polym. Chem.*, 2015, **53**, 2510–2516.
33 H. W. Lee, Y. Yoon, S. Park, J. H. Oh, S. Hong, L. S. Liyanage, H. L. Wang, S. Morishita, N. Patil, Y. J. Park, J. J. Park, A. Spakowitz, G. Galli, F. Gygi, P. H.-S. S. Wong, J. B.-H. H. Tok, J. M. Kim and Z. A. Bao, *Nat. Commun.*, 2011, **2**, 541.
34 S. K. Samanta, M. Fritsch, U. Scherf, W. Gomulya, S. Z. Bisri and M. A. Loi, *Acc. Chem. Res.*, 2014, **47**, 2446–2456.
35 A. Nish, J.-Y. Hwang, J. Doig and R. J. Nicholas, *Nat. Nanotechnol.*, 2007, **2**, 640–646.
36 F. Lemasson, N. Berton, J. Tittmann, F. Hennrich, M. M. Kappes and M. Mayor, *Macromolecules*, 2012, **45**, 713–722.
37 N. A. Rice, A. V. Subrahmanyam, B. R. Coleman and A. Adronov, *Macromolecules*, 2015, **48**, 5155–5161.
38 H. Wang and Z. Bao, *Nano Today*, 2015, **10**, 737–758.
39 J.-Y. Hwang, A. Nish, J. Doig, S. Douven, C.-W. Chen, L.-C. Chen and R. J. Nicholas, *J. Am. Chem. Soc.*, 2008, **130**, 3543–3553.
40 A. Nish, J.-Y. Hwang, J. Doig and R. J. Nicholas, *Nanotechnology*, 2008, **19**, 095603.
41 Y. Chen, W. Huang, C. Li and Z. Bo, *Macromolecules*, 2010, **43**, 10216–10220.
42 J. Murage, J. W. Eddy, J. R. Zimbalist, T. B. McIntyre, Z. R. Wagner and F. E. Goodson, *Macromolecules*, 2008, **41**, 7330–7338.
43 P. Imin, M. Imit and A. Adronov, *Macromolecules*, 2012, **45**, 5045–5050.
44 S. M. Bachilo, M. S. Strano, C. Kittrell, R. H. Hauge, R. E. Smalley and R. B. Weisman, *Science*, 2002, **298**, 2361–2366.
45 S. K. Doorn, D. A. Heller, P. W. Barone, M. L. Usrey and M. S. Strano, *Appl. Phys. A*, 2004, **78**, 1147–1155.
46 M. S. Strano, M. Zheng, A. Jagota, G. B. Onoa, D. A. Heller, P. W. Barone and M. L. Usrey, *Nano Lett.*, 2004, **4**, 543–550.
47 M. S. Strano, S. K. Doorn, E. H. Haroz, C. Kittrell, R. H. Hauge and R. E. Smalley, *Nano Lett.*, 2003, **3**, 1091–1096.
48 S. Brown, A. Jorio, P. Corio, M. Dresselhaus, G. Dresselhaus, R. Saito and K. Kneipp, *Phys. Rev. B*, 2001, **63**, 1–8.
49 M. S. Strano, C. A. Dyke, M. L. Usrey, P. W. Barone, M. J. Allen, H. Shan, C. Kittrell, R. H. Hauge, J. M. Tour and R. E. Smalley, *Science*, 2003, **301**, 1519–1522.
50 D. A. Heller, P. W. Barone, J. P. Swanson, R. M. Mayrhofer and M. S. Strano, *J. Phys. Chem. B*, 2004, **108**, 6905–6909.
51 R. B. Weisman and S. M. Bachilo, *Nano Lett.*, 2003, **3**, 1235–1238.
52 M. W. Schmidt, K. K. Baldridge, J. Boatz, S. Elbert, M. S. Gordon, J. H. Jensen, S. Koseki, N. Matsunaga, K. A. Nguyen,

S. Su, T. L. Windus, M. Dupuis and J. A. Montgomery, *J. Comput. Chem.*, 1993, **14**, 1347–1363.

Graphical Abstract

Nitration of a poly(fluorene-*co*-phenylene) backbone influences its selectivity for semiconducting versus metallic single-walled carbon nanotubes, and the regiochemistry of the nitro group has a significant impact.